Mössbauer effect and magnetization studies of Er - Fe - B permanent magnetic materials

1997 J. Phys.: Condens. Matter 9 2645

(http://iopscience.iop.org/0953-8984/9/12/011)

J. Phys.: Condens. Matter **9** (1997) 2645–2656. Printed in the UK PII: S0953-8984(97)77475-7

Mössbauer effect and magnetization studies of Er–Fe–B permanent magnetic materials

M Manivel Raja and A Narayanasamy†

Department of Nuclear Physics, University of Madras, Guindy Campus, Madras 600 025, India

Received 30 August 1996, in final form 10 December 1996

Abstract. Mössbauer and saturation magnetization studies have been carried out at room temperature on $Er_{2-x}Y_xFe_{14}B$ and $Er_2Fe_{14-x}Si_xB$ permanent magnetic materials with $x = 0.0, 0.5, 1.0, 1.5$ and 2.0. A simple charge transfer from the rare-earth sublattice to the 3d band of iron accounts for the observed increase in the saturation magnetization and ^{57}Fe hyperfine field with the substitution of Y for Er. This can also be explained on the basis of the reduction in the strength of the Er–Fe negative exchange interaction and an increase in the Fe–Fe exchange interaction strength due to lattice expansion on Y substitution. The decrease in the saturation magnetization and the ^{57}Fe hyperfine field when Fe is partially replaced by Si is attributed to the reduction in the number of Fe neighbours and also to the reduction in the Fe magnetic moment due to an effective charge transfer from Si to the Fe 3d band. The Fe sublattice magnetization is found to be slightly affected by the type of rare-earth ion in the rare-earth sublattice.

1. Introduction

The exotic magnetic properties of the $Nd_2Fe_{14}B$ intermetallic compound have created the interest for an extensive study on high-performance magnetic materials [1–3]. A huge magnetocrystalline anisotropy of this system arises from the rare-earth sublattice due to its large orbital magnetic moment. In $R_2Fe_{14}B$ compounds where R stands for rare earth, all of the light rare-earth atoms couple ferromagnetically while all of the heavy rare-earth atoms couple antiferromagnetically with the Fe sublattice [4]. Even though all of the rare earths from Ce to Y form the $R_2Fe_{14}B$ hard magnetic phase, only Nd and Pr compounds exhibit the highest saturation magnetization, energy product and magnetocrystalline anisotropy, and hence these compounds are mostly used for high-performance applications in the permanent magnet industry. The magnetic properties of $R_2Fe_{14}B$ compounds have been extensively studied by many investigators, as reviewed by Buschow [5] and Herbst [6]. The saturation magnetization of the $Er_2Fe_{14}B$ compound is found to be low due to the ferrimagnetic configuration of Er and Fe sublattices even though the Er sublattice magnetization is high. Also, the thermomagnetization curve shows a spin-reorientation transition temperature at 330 K due to the competition between the planar and axial anisotropies of the rare-earth and iron sublattices respectively [7]. Our earlier work [8] reports the effect of substitution of non-magnetic elements Y and Si in the R and Fe sublattices respectively on the spin-reorientation transition temperature of the $Er_2Fe_{14}B$ compound. Mössbauer effect studies [9, 10] reveal that the Fe hyperfine field (H_{hf}) is linearly proportional to the Fe local magnetic

† Address for correspondence: Professor A Narayanasamy, Department of Nuclear Physics, University of Madras, Guindy Campus, Madras 600 025, India. E-mail: madphy@iitm.ernet.in.

0953-8984/97/122645+12$19.50

Table 1. Mössbauer effect parameters (hyperfine magnetic fields (H_{hf}), quadrupole splittings (Q.S.), isomer shifts (I.S.)) of the $Er_{2-x}Y_xFe_{14}B$ (series A) compounds at room temperature.

		Fe sites						
Mössbauer parameter	x	$8j_1$	$8j_2$	$16k_1$	$16k_2$	4c	4e	Average
H_{hf}	0.0	264	304	276	293	271	247	280.5
(kOe)	0.5	256	321	274	287	281	253	280.9
	1.0	258	325	275	287	282	255	282.2
	1.5	256	327	280	290	283	257	284.7
	2.0	267	334	284	294	283	261	289.9
Q.S.	0.0	−0.18	−0.29	0.02	−0.09	−0.80	0.06	
(mm s^{-1})	0.5	0.18	0.34	0.17	0.08	−0.81	0.30	
	1.0	0.28	0.56	0.25	0.16	−0.81	0.27	
	1.5	0.24	0.62	0.26	0.16	−0.61	0.28	
	2.0	0.29	0.47	0.25	0.17	−0.56	0.29	
I.S.[a]	0.0	0.05	0.12	−0.06	−0.10	0.07	−0.08	−0.022
(mm s^{-1})	0.5	−0.03	0.10	−0.02	−0.09	−0.04	−0.01	−0.025
	1.0	−0.02	0.09	−0.01	−0.08	−0.05	−0.05	−0.026
	1.5	−0.04	0.08	−0.02	−0.09	−0.02	−0.03	−0.029
	2.0	−0.06	0.09	−0.03	−0.08	−0.06	−0.02	−0.033

[a]The isomer shift is relative to (the isomer shift of) natural iron at room temperature.

moment. But band-structure calculations [11] show that there is a deviation from the linear relationship between the Fe hyperfine field and local magnetic moment in the $R_2Fe_{14}B$ compounds. However, Long *et al* [12] have suggested that the theoretically calculated hyperfine fields must be treated with caution.

In this work a detailed study has been carried out, using Mössbauer spectroscopy and magnetization measurements, with the aim of achieving an understanding of the hyperfine interactions in the $Er_2Fe_{14}B$ compound caused by modifying the rare-earth and iron sublattices with non-magnetic elements.

2. Experimental procedure

The specimens under investigation (series A: $Er_{2-x}Y_xFe_{14}B$ and series B: $Er_2Fe_{14-x}Si_xB$ where $x = 0.0$, 0.5, 1.0, 1.5 and 2.0) were prepared by induction melting the constituent elements in vacuum as reported in our earlier work [8]. The phase purity of the compounds was checked by the x-ray powder diffraction technique using a high-resolution Guinier-type x-ray powder diffractometer with a primary quartz monochromator to select Cu $K\alpha_1$ radiation. Magnetization measurements were performed for the polycrystalline samples in applied magnetic fields up to a maximum of 16 kOe using a vibrating-sample magnetometer. The Mössbauer effect experiment was carried out at room temperature using a constant-acceleration Mössbauer spectrometer in transmission mode with a 50 mCi ^{57}Co(Rh) gamma-ray source. The Mössbauer spectrometer was calibrated with a standard natural iron foil of thickness 20 μm before and after the measurements.

Table 2. Mössbauer effect parameters (hyperfine magnetic fields (H_{hf}), quadrupole splittings (Q.S.), isomer shifts (I.S.) and relative intensities) for the $Er_2Fe_{14-x}Si_xB$ (series B) compounds at room temperature.

		Fe sites						
Mössbauer parameter	x	$8j_1$	$8j_2$	$16k_1$	$16k_2$	4c	4e	Average
H_{hf}	0.0	264	304	276	293	271	247	280.5
(kOe)	0.5	246	290	260	285	257	226	265.5
	1.0	224	275	227	253	256	202	243.4
	1.5	219	269	224	248	239	191	234.5
	2.0	200	252	207	230	223	177	219.4
Q.S.	0.0	−0.18	−0.29	0.02	−0.09	−0.80	0.06	
(mm s^{-1})	0.5	−0.20	−0.31	−0.13	−0.07	−0.60	0.07	
	1.0	−0.12	−0.22	−0.09	−0.03	−0.57	0.18	
	1.5	−0.13	−0.27	−0.08	−0.01	−0.54	0.17	
	2.0	−0.17	−0.19	−0.12	−0.02	−0.42	0.19	
I.S.[a]	0.0	0.05	0.12	−0.06	−0.10	0.07	−0.08	−0.022
(mm s^{-1})	0.5	0.08	0.11	−0.09	−0.08	0.15	0.02	−0.010
	1.0	0.11	0.12	−0.09	−0.06	0.20	0.03	0.006
	1.5	0.15	0.10	−0.06	−0.08	0.15	0.02	0.008
	2.0	0.14	0.15	−0.05	−0.07	0.17	0.03	0.022
	0.0	14.3	14.3	28.6	28.6	7.1	7.1	
Intensity	0.5	16.0	14.6	27.0	26.0	7.8	8.6	
(%)	1.0	16.4	15.0	26.0	25.0	9.0	8.6	
	1.5	16.7	14.7	25.8	25.2	9.4	8.2	
	2.0	16.7	14.9	26.0	25.5	9.5	8.4	

[a]The isomer shift is relative to (the isomer shift of) natural iron at room temperature.

3. Results

The x-ray powder diffraction analysis was carried out for all of the compounds in series A and B, and it shows that all of them crystallized into a tetragonal phase with the space group $P4_2/mnm$. No line corresponding to any impurity phase was detected. ^{57}Fe Mössbauer spectra recorded at room temperature for the two series of compounds are shown in figures 1(a) and 1(b). In the figures the dots represent the experimental spectrum and the continuous solid lines are results from the least-squares fitting of the experimental data using the method of Bent *et al* [13]. The Mössbauer spectra were analysed using six sextets corresponding to the six inequivalent Fe sites. The relative intensities of the six sextets corresponding to the j_1, j_2, k_1, k_2, c and e iron sites for the $Er_2Fe_{14}B$ and Y-substituted compounds were constrained to the ratio 8:8:16:16:4:4 on the basis of the Fe site occupancy [3] whereas they were obtained by iteration for the Si-substituted compounds. It was assumed that the recoilless fractions were the same for all of the Fe sites and for all of the compounds. Also, the relative intensities of the six lines in each sextet were assumed to be in the ratio 3:2:1:1:2:3, as powder samples were used for the absorber preparation. The assignment of six subspectra to the various Fe sites was done on the basis of their relative intensities and also by taking into account not only the number of Fe neighbours but also the number of Nd and B neighbours to an Fe atom [12]. The Mössbauer parameters (hyperfine magnetic fields, isomer shift, quadrupole splitting, etc) as obtained from the least-squares fitting

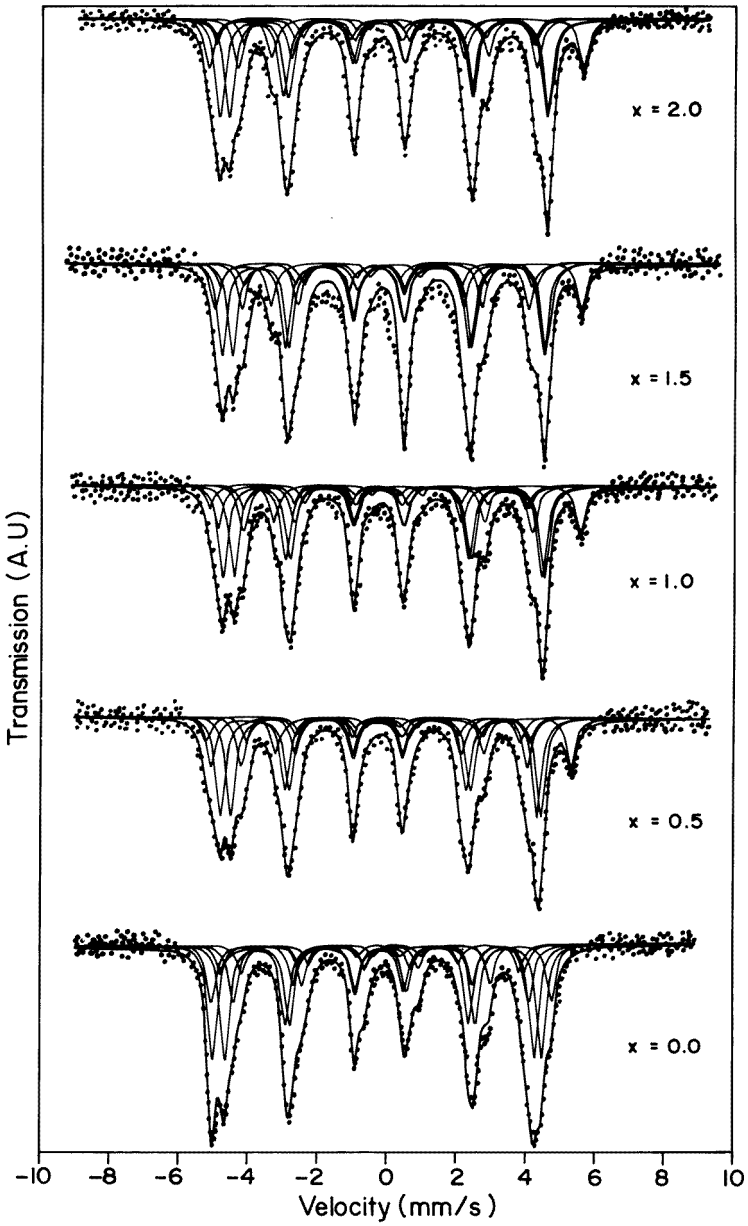

(a)

Figure 1. (a) ^{57}Fe Mössbauer spectra of the $Er_{2-x}Y_xFe_{14}B$ compounds with $x = 0.0$, 0.5, 1.0, 1.5 and 2.0 at room temperature. (b) ^{57}Fe Mössbauer spectra of the $Er_2Fe_{14-x}Si_xB$ compounds with $x = 0.0$, 0.5, 1.0, 1.5 and 2.0 at room temperature.

of the spectra are given in tables 1 and 2. The accuracy of the hyperfine-magnetic-field values is estimated to be ± 1.4 kOe and that of the quadrupole splitting is estimated to be ± 0.032 mm s^{-1}. The variation of the weighted-average Fe hyperfine field with the Y and Si concentrations is shown in figure 2. It is found that the weighted-average Fe hyperfine

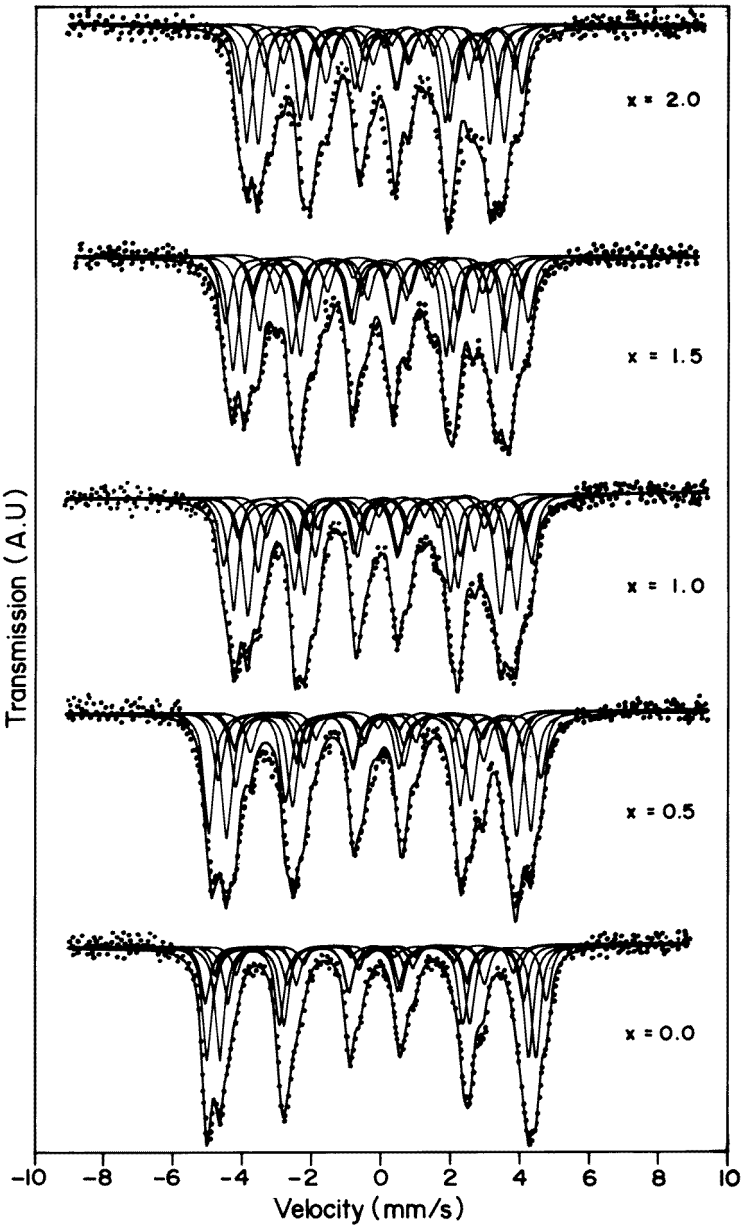

(b)

Figure 1. (Continued)

field increases with the Y concentration and drastically decreases with the Si concentration. A similar variation is also found with magnetic moment as discussed later, in section 4.2. The weighted-average isomer shift is also determined for all of the compounds, and the values are given in tables 1 and 2. The accuracy of the isomer shift values is estimated to be ± 0.002 mm s^{-1}. The dependence of the weighted-average isomer shift on the Y and Si

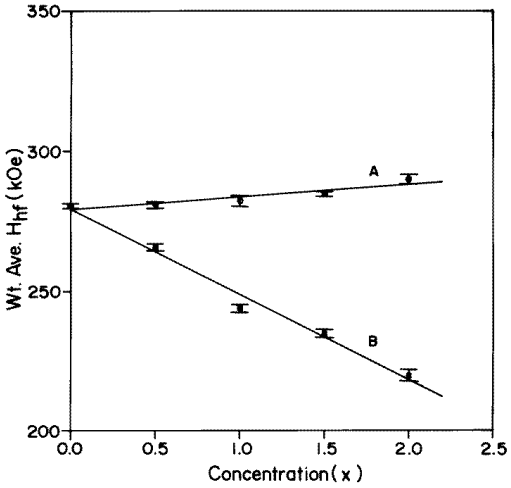

Figure 2. The dependence of the weighted-average Fe hyperfine fields of the $Er_{2-x}Y_xFe_{14}B$ (series A) and $Er_2Fe_{14-x}Si_xB$ (series B) compounds on the Y and Si concentrations. (The solid lines are the straight-line fits of the experimental data.)

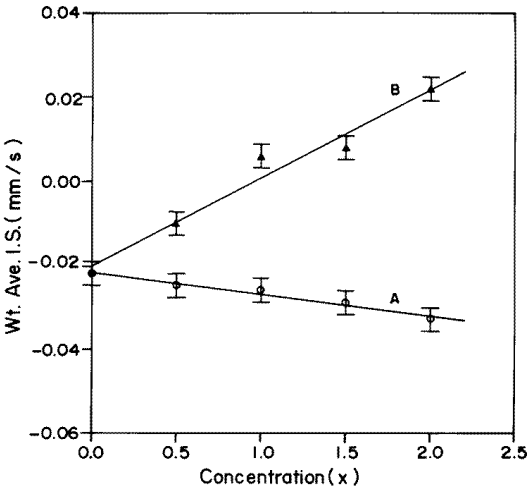

Figure 3. The variation of the weighted-average isomer shift of the $Er_{2-x}Y_xFe_{14}B$ (series A) and $Er_2Fe_{14-x}Si_xB$ (series B) compounds with the Y and Si concentrations. (The solid lines are the straight-line fits of the experimental data.)

concentrations is shown in figure 3, and it shows that the isomer shift decreases with the Y concentration and increases with the Si concentration. The mechanism for the variation of the weighted-average Fe hyperfine field, isomer shift and quadrupole splitting with Y and Si substitution is discussed in section 4.

The magnetic measurements were made on polycrystalline samples with applied magnetic fields up to 16 kOe at room temperature. The magnetization curves of all of the samples of series A and B are shown in figures 4(a) and 4(b). The saturation magnetization was calculated by extrapolating the high-field part of the magnetization curves, and the

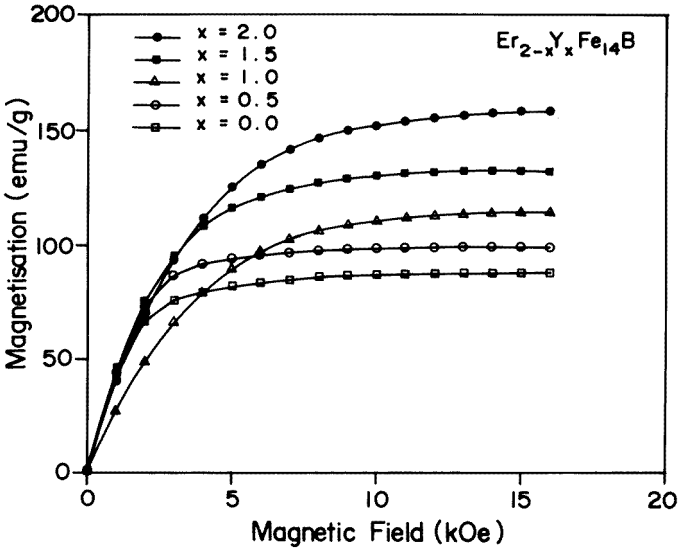

(a)

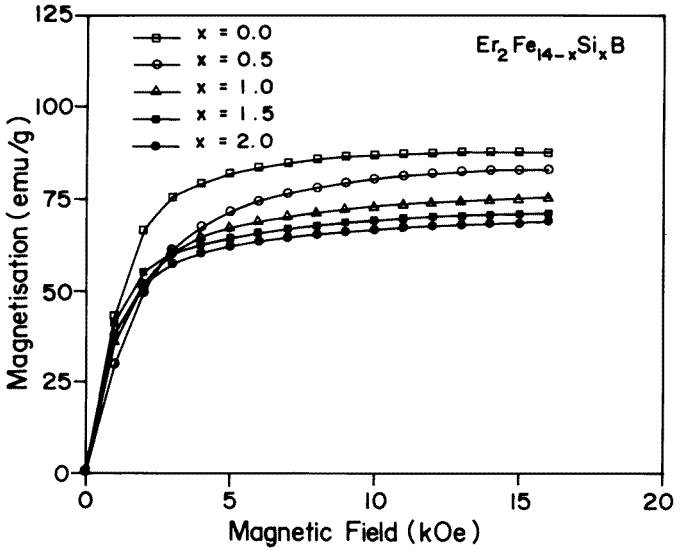

(b)

Figure 4. (a) Magnetization curves of the $Er_{2-x}Y_xFe_{14}B$ compounds with $x = 0.0$, 0.5, 1.0, 1.5 and 2.0 at room temperature. (b) Magnetization curves of the $Er_2Fe_{14-x}Si_xB$ compounds with $x = 0.0$, 0.5, 1.0, 1.5 and 2.0 at room temperature.

values are given in table 3. The Fe sublattice magnetization was calculated from Mössbauer studies using the correlation between the observed Fe hyperfine magnetic field and the Fe magnetic moment, i.e. 1 μ_B = 147 kOe. The rare-earth sublattice magnetization was estimated by subtracting the Fe sublattice magnetization from the saturation magnetization of the compound at room temperature. From the table we see that the Fe sublattice

Table 3. The saturation magnetizations (σ_s and M_s) and the rare-earth and the iron sublattice magnetizations (μ_R and μ_{Fe}) of the $Er_{2-x}Y_xFe_{14}B$ (series A) and $Er_2Fe_{14-x}Si_xB$ (series B) compounds at room temperature.

Compounds	x	σ_s (emu g^{-1})	M_s (μ_B/f.u.)	μ_{Fe} (μ_B/f.u.)[a]	μ_R (μ_B/f.u.)
Series A	0.0	88.0	17.8	26.7	−8.9
	0.5	99.5	19.4	26.8	−7.4
	1.0	114.2	21.5	26.9	−5.4
	1.5	132.0	23.9	27.1	−3.2
	2.0	158.5	27.5	27.6	0.0
Series B	0.0	88.0	17.8	26.7	−8.9
	0.5	83.2	16.5	25.3	−8.8
	1.0	76.0	15.0	23.2	−8.2
	1.5	71.0	13.8	22.3	−8.5
	2.0	68.2	12.9	20.9	−8.0

[a] Calculated from the observed hyperfine magnetic fields.

magnetization calculated from the observed hyperfine magnetic field was found to be almost equal to the saturation magnetization of the $Y_2Fe_{14}B$ compound. This confirms that the magnetic moment of $Y_2Fe_{14}B$ arises only from the Fe sublattice. Hence the subtraction of the Fe sublattice magnetization from the saturation magnetization gives the value of the rare-earth sublattice magnetization at room temperature in the case of the other compounds. The saturation magnetization increases with Y concentration and decreases with Si concentration as shown in figure 5.

4. Discussion

A combined study of the magnetic and Mössbauer measurements of the series A and B compounds leads to some important conclusions on the various factors that contribute to the effective Fe hyperfine field in the Y- and Si-substituted $Er_2Fe_{14}B$ compounds. The effect of non-magnetic-element substitution in the rare-earth and iron sublattices on hyperfine parameters such as the hyperfine field, quadrupole splitting and isomer shift is discussed in the following section.

4.1. Mössbauer spectroscopy

4.1.1. The hyperfine interaction. From figures 1(a) and 1(b) we observe that the positions of the satellite peaks are slightly shifted to the higher-velocity side for the Y-substituted compounds, and that the spacings between the outermost peaks of the spectra are reduced for the Si-substituted compounds. This indicates that the substitution of Y for Er increases and of Si for Fe decreases the Fe hyperfine field in the $Er_2Fe_{14}B$ compound. Mössbauer studies on $R_2Fe_{14}B$ compounds [14] reveal that the average iron hyperfine field increases as R varies from La to Gd and decreases for rare-earth atoms heavier than Gd. This implies that the antiferromagnetic interaction between the heavier rare-earth atoms and iron atoms reduces the ^{57}Fe hyperfine field. We find from table 3 that the Fe sublattice magnetization decreases and from table 1 that the isomer shift increases with the increase of Er concentration. This could happen if there was an additional charge transfer, probably from the 5p orbitals of the Er atom to the 3d shell of the Fe atom. This would reduce the Fe magnetic moment and

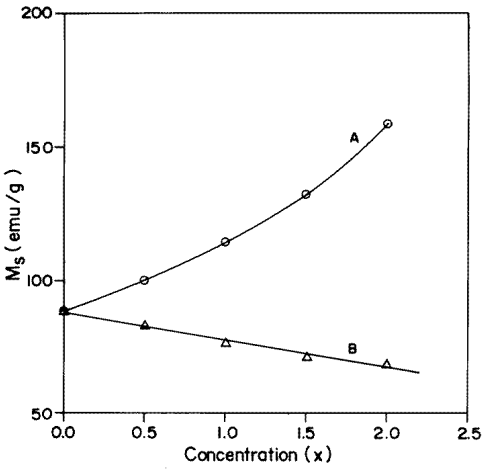

Figure 5. The dependence of the saturation magnetization of the $Er_{2-x}Y_xFe_{14}B$ (series A) and $Er_2Fe_{14-x}Si_xB$ (series B) compounds on the Y and Si concentrations at room temperature. (The solid lines are a guide for the eyes for curve A and the straight-line fit for curve B.)

increase the isomer shift due to the increase in the shielding of the 3s electrons by the 3d electrons. Such a charge transfer has been predicted by Herbst [6] in the case of $R_2Fe_{14}B$ systems and by Ying-Chang Yang *et al* [15] in the case of $RTiFe_{11}N_{1-\delta}$ compounds. Since Y does not have 5p electrons, the substitution of Y in the place of Er leads to an increase in the Fe magnetic moment. The substitution of Y for Er reduces the strength of the Er–Fe negative exchange interaction and also enhances the strength of the Fe–Fe interaction by increasing the Fe–Fe interatomic distance on lattice expansion. This will also contribute to the observed increase of H_{hf} for Fe on Y substitution.

For the Si-substituted compounds, the average Fe H_{hf} decreases at a rate of 30.7 kOe per Si atom. The decrease of H_{hf} at the Fe atom indicates that the local atomic environment at the Fe site is affected by the reduction in the number of Fe near-neighbour atoms. Ge *et al* [16] have deduced that the existence of a nearest Fe neighbour leads to an increase in the Fe H_{hf} of about 15 kOe per Fe atom in the case of the $Nd_2Fe_{14}B$ compound. According to this observation one can expect that the substitution of Si for Fe will decrease the Fe H_{hf} at a rate of 15 kOe per Si atom, whereas the observed reduction in the Fe H_{hf} is larger by a factor of 2. This implies that the decrease in the Fe H_{hf} is to be attributed not only to the reduction in the number of nearest Fe neighbours but also to the reduction in the Fe magnetic moment caused by the substituent atom. A similar variation is also observed in the saturation magnetization of the $Er_2Fe_{14-x}Si_xB$ compounds at room temperature.

The variation of the relative intensities of the sextets as seen from table 2 shows that Si prefers to occupy the $16k_2$ and $16k_1$ Fe sites. The $8j_1$ Fe site has two $16k_2$ nearest Fe neighbours [17] with the Fe–Fe interatomic distance less than 2.45 Å, which gives rise to the antiferromagnetic exchange interaction between them. When Si occupies the $16k_2$ site, the antiferromagnetic Fe–Fe couplings are broken and hence the Curie temperature is expected to increase. Our earlier study [8] shows an increase of the Curie temperature with Si substitution. The earlier Mössbauer studies report that Si occupies $16k_2$ sites only [18] or both $8j_1$ and $16k_2$ sites [19]. However, neutron diffraction studies [19] have shown that Si substitutes at 4c, $8j_1$ and $16k_2$ sites in the $N_2Fe_{14}B$ compound. Thus there is a consensus among various studies at least with respect to the occupation of $16k_2$ sites by Si.

4.1.2. The quadrupole splitting. The Mössbauer spectra were analysed on the assumption that the principal component of the electric field gradient is axially symmetric at all Fe sites. The electric quadrupole interaction was treated as a first-order perturbation on the magnetic dipole interaction. As seen from tables 1 and 2 there is a considerable change in the quadrupole splitting at the 4c site with Y and Si substitution, implying that the symmetry at the 4c site is very much affected when rare-earth and iron sublattices are substituted for with Y and Si respectively.

4.1.3. The isomer shift. The isomer shift depends on the s-electron density and the interatomic distance between near neighbours. Our earlier study [8] shows that the replacement of Er by Y in the $Er_2Fe_{14}B$ compound leads to the lattice expansion and hence to an increase in the near-neighbour distance. The lattice expansion results in the spatial expansion of Fe atomic orbitals, and so one can expect a decrease in the s-electron density at the Fe nucleus and hence an increase in the value of the isomer shift. As discussed in section 4.1.1, any additional charge transfer from an Er atom to the 3d band of an Fe atom will increase the isomer shift with increasing Er concentration; in other words, the isomer shift will decrease with the increase of the Y concentration. As a result one should expect an increase in isomer shift on lattice expansion and a decrease with the reduction in the charge transfer from the rare-earth sublattice to the Fe 3d band when Er is substituted for with Y. The resultant change in the isomer shift is due to the competition between these two mechanisms. Figure 3 shows that the isomer shift decreases with the increase of the Y concentration, and the change is found to be very small, 0.005 mm s^{-1} per Y atom, because of the above two competing mechanisms. In the case of series B compounds, the substitution of Si for Fe decreases the unit-cell volume, which results in the decrease of the interatomic distance between near neighbours. So, the isomer shift is expected to decrease due to the increase of the s-electron density at the Fe sites. But the isomer shift was found to increase at a rate of 0.021 mm s^{-1} per Si atom which can be explained on the basis of an effective charge transfer from the non-magnetic Si atom to the Fe 3d band which will increase the screening of the 3s-electron density at the Fe nucleus. This explanation is also supported by the observed reduction in the Fe magnetic moment in $Er_2Fe_{14-x}Si_xB$ compounds as discussed in the following section.

4.2. Magnetization measurements

In the Y-substituted compounds, the saturation magnetization is found to increase with the Y concentration at a rate of approximately 5 μ_B per Y atom. This results from the formation of a Y–Fe bond replacing the antiferromagnetic Er–Fe coupling. The experimental value of the saturation magnetization of $Y_2Fe_{14}B$ at room temperature is 27.5 μ_B/f.u. which corresponds to 1.96 μ_B per Fe atom. The Fe magnetic moment, as calculated from the Fe hyperfine field, also slightly increases when the antiferromagnetic Er is replaced with Y as seen from table 3. This reveals that the Fe sublattice magnetization is slightly influenced by the 3d–4f magnetic interaction. As already discussed in section 4.1 the additional charge flow from the Er to the Fe 3d band is responsible for the slight decrease of the Fe magnetic moment with the increase of the Er concentration. The average Er magnetic moment in the $Er_2Fe_{14}B$ compound was found to be 4.45 μ_B, which is somewhat larger than the value of 3.55 μ_B calculated from the neutron diffraction measurements [20]. In the case of Si-substituted compounds, the saturation magnetization decreases with increasing Si concentration. The rate of decrease is 2.9 μ_B per Si atom, and this is higher than 1.91 μ_B which one would expect on the basis of the replacement of an Fe atom by a non-magnetic Si atom alone. This

indicates that the decrease in magnetization is not only due to the replacement of Fe atoms by non-magnetic Si atoms but also to the reduction in the Fe magnetic moment caused by the substituent atoms.

5. Conclusions

(i) The Mössbauer studies of $Er_{2-x}Y_xFe_{14}B$ show that the weighted-average Fe hyperfine field increases with the Y substitution. Charge transfer from the rare earth to the Fe 3d band, the decrease in the strength of the antiferromagnetic Er–Fe interaction due to the formation of Y–Fe coupling, and the increase in the strength of the ferromagnetic Fe–Fe interaction occurring because of the increase in the interatomic distance on Y substitution are responsible for this observation.

(ii) The weighted-average Fe hyperfine field in $Er_2Fe_{14-x}Si_xB$ decreases at a rate of 30.7 kOe per Si atom. This is attributed to the reduction in the number of nearest Fe neighbours and also to the reduction in the Fe magnetic moment.

(iii) The change in isomer shift with Y concentration is attributed to the combined effect of the lattice expansion and the reduction in the charge transfer from the rare-earth sublattice to the Fe 3d band. The increase in the value of the isomer shift with Si substitution is explained on the basis of charge transfer from the Si to the Fe atom.

(iv) The symmetry at the 4c site is found to be affected very substantially as seen from the variation in the quadrupole splitting with Y and Si substitution.

(v) The saturation magnetization of $Er_2Fe_{14}B$ increases with the degree of substitution of Y for Er, and decreases with the degree of substitution of Si for Fe. The magnetization of the Fe sublattice is found to be slightly dependent on the type of rare-earth atom in the rare-earth sublattice.

Acknowledgments

This work was supported by the Council of Scientific and Industrial Research (CSIR), Government of India, under the research scheme No 4(114)/91-EMR-II, and also by the University Grants Commission (UGC), India, under the Special Assistance Programme (SAP). The authors would like to thank Professor T Nagarajan for his interest in this work and Mr B Soundarajan and Mr K Ravichandran for their technical assistance. One of the authors (MMR) would like to thank the CSIR for the award of a Senior Research Fellowship during the course of this work.

References

[1] Sagawa M, Fujimura S, Togawa N, Yamamoto H and Mutsuura Y 1984 *J. Appl. Phys.* **55** 2083
[2] Croat J J, Herbst J F, Lee R W and Pinkerton F E 1984 *J. Appl. Phys.* **55** 2078
[3] Herbst J F, Croat J J, Pinkerton F E and Yelon W B 1984 *Phys. Rev.* B **29** 4176
[4] Huang M O, Oswald E, Boltich E, Hirosawa S, Wallace W E and Schwab E 1985 *Physica* B **130** 319
[5] Buschow K H J 1991 *Rep. Prog. Phys.* **54** 1123
[6] Herbst J F 1991 *Rev. Mod. Phys.* **63** 819
[7] Hirosawa S and Sagawa M 1985 *Solid State Commun.* **54** 335
[8] Manivel Raja M and Narayanasamy A 1996 *J. Alloys Compounds* **233** 140
[9] Van Noort H M, De Mooij D B and Buschow K H J 1985 *J. Appl. Phys.* **57** 5414
[10] Gubbens P C M, Van Apeldoorn J H J, Van der Kraan A M and Buschow K H J 1974 *J. Phys. F: Met. Phys.* **4** 921
[11] Hummler K, Beuerle T and Fahnle M 1992 *J. Magn. Magn. Mater.* **115** 207

[12] Long G J, Grandjean F and Pringle O A 1993 *J. Magn. Magn. Mater.* **125** L29
[13] Bent M F, Persson B and Agresti D G 1969 *Comput. Phys. Commun.* **1** 67
[14] Long G J, Kulasekere R, Pringle O A, Grandjean F and Buschow K H J 1992 *J. Magn. Magn. Mater.* **117** 239
[15] Yang Ying-chang, Zhang Xiao-dong, Ge Sen-lin, Pan Qi, Kong Lin-shu, L Hailin, Yang Ji-lian, Zhang Bai-Sheng, Ding Yong-fan and Ye Chun-tang 1991 *J. Appl. Phys.* **70** 6001
[16] Ge S H, Zhang Y D, Li F S, Budnick J I and Panissod P 1992 *J. Magn. Magn. Mater.* **116** 211
[17] Givord D, Li H S and Moreau J M 1984 *Solid State Commun.* **50** 497
[18] Li Z W, Zhou X Z and Morrish A H 1990 *Phys. Rev.* B **41** 8617
[19] Marasinghe G K, Pringle O A, Long G J, James W J, Xie D, Li J, Yelon W B and Grandjean F 1993 *J. Appl. Phys.* **74** 6798
[20] Yelon W B and Herbst J F 1986 *J. Appl. Phys.* **59** 93